

Study of the Plasma-Wall Interface – Measurement and Simulation of Sheath Potential Profiles

Samuel J. Langendorf¹ and Mitchell L. R. Walker²
High-Power Electric Propulsion Laboratory, Georgia Institute of Technology
Atlanta, GA 30332 USA

Laura P. Rose³ and Michael Keidar⁴
Micropropulsion and Nanotechnology Laboratory, George Washington University
Washington, D.C. 20052 USA

and

Lubos Brieda
Particle in Cell Consulting LLC, Falls Church, VA 22046

Limitations in power density and specific mass of electric propulsion devices are imposed by interactions of the plasma with the confining wall material. In this investigation, potential profiles of plasma sheaths over boron nitride (BN) and alumina samples are experimentally measured and compared to the results of theoretical prediction and simulation. Plasmas are generated in a multidipole device at argon pressures of 5×10^{-5} to 1×10^{-4} Torr-Ar by means of energetic electrons injected from negatively-biased emissive filaments. Electron temperatures and densities are measured using a cylindrical Langmuir probe and range from 0.95 – 2.15 eV and 1.8×10^{14} – 4.6×10^{14} m⁻³, respectively. Sheath thickness range from approximately 20 mm to approximately 40 mm. Simulations performed of the experimental plasmas using the Starfish plasma simulation code predict potential profiles in nominal agreement with the measurements. The shape of the sheath profiles over the alumina samples changes as the bias voltage of the emissive filaments is varied, transitioning from a nominal ion sheath profile when the filament bias is -60 V to an electron sheath when the filament bias is -120 V. When the alumina sample is at a comparable condition to the BN, the measured sheath thickness is approximately 33% of that of the BN sample, the potential difference across the sheath is 22% of that of the BN sample, and the near wall electric field strength is approximately 10% of that of the BN sample. It is expected that for a simulation to reproduce the alumina results, it will need to incorporate the effect of secondary electron emission from the wall surface.

I. Introduction

To increase the thrust-to-power ratio of electric propulsion devices for spacecraft, it is necessary to increase the ion number density of the discharge plasma for a given power. It has been observed that the ion number density in Hall-effect thruster (HET) discharge plasmas does not increase with power beyond a certain threshold due to the interaction between the discharge plasma and the discharge channel wall and the resulting behavior of the plasma sheath¹. In Ref. 2, this effect is shown to be linked to secondary electron emission (SEE) from the wall material of the discharge channel. Recent simulation studies³ show that the emitted electrons modify the plasma sheath and cause increased power deposition to the discharge channel wall, motivating the present study, which seeks to provide experimental measurements and validated simulation capability for wall material effects on plasma sheaths.

¹ Graduate Research Assistant, Aerospace Engineering, 270 Ferst Dr. NW, Student Member AIAA

² Associate Professor, Aerospace Engineering, 270 Ferst Dr. NW, Associate Fellow AIAA

³ Graduate Research Assistant, Mechanical and Aerospace Engineering, Student Member AIAA

⁴ Associate Professor, Mechanical and Aerospace Engineering, 801 22nd Street NW, Senior Member AIAA

Plasma sheaths are non-quasineutral regions that form at interactions between plasmas and physical boundaries. The existence and importance of plasma sheaths has been recognized since the early 1900's, and the theoretical study of plasma sheath properties has seen considerable development. In recent years, sheaths have received renewed attention as an area in need of investigation, particularly in regard to the need to obtain experimental measurements to support the theoretical models.⁴ With the advent of modern computing and plasma simulation capability, experimental observation of sheaths can also serve to validate the results of plasma simulations. In the current experiment, experimental measurements and simulations are compared for multiple materials with different SEE yields to take steps towards that objective.

II. Setup

Experiments are conducted at the Georgia Institute of Technology and simulations are conducted at the George Washington University.

A. Experiment

A multipole plasma device was constructed in which to investigate the effect of high-energy electrons and other sheath phenomena. Multipole devices have been used in many experiments since their invention in the early 1970's as a way to generate quiescent and spatially uniform plasmas⁵⁻⁸. The device consists of a cylindrical aluminum cage lined with permanent magnets which generate a magnetic field that confines ionizing electrons generated by emissive filaments within the device. The filaments are biased below ground and below the plasma to impart energy to the thermionically-emitted electrons. Neutral molecules enter the device from the vacuum chamber, which receives a mass flow input several meters distant from the device to allow the gas to expand throughout the chamber and enter the plasma cell with a spatially uniform number density.

Figure 1 shows a schematic of the plasma device. The cage interior length is 36 in and the interior diameter is 24 in. There are 24 rails of 1/8 in thick aluminum u-channel that form the exterior of the cylindrical cage, each lined with 11 ceramic CM-0411 permanent magnets. The magnets are all oriented with the same polarity on each rail with adjacent rails assigned opposing polarities – the 'broken line cusp' configuration described by Leung *et al.*⁹. The magnets are equally spaced 3.5 inches apart on center along the rails. The end plates are 24 inch aluminum squares, 1/4 inch thick, with 1/2 inch holes drilled in a 1.725 by 3.175 inch grid to increase neutral gas flow into the plasma region. A grid of similarly spaced and polarized magnets is held on the interior of the each of the end plates with u-channel. Five thoriated tungsten filaments of length 2.5 inch and diameter 0.006 inch are resistively heated in parallel to generate the electrons that create the plasma. The filaments are positioned in the center of the plasma using 1/4 inch OD alumina tubing.

The plasma device is operated in the Georgia Institute of Technology Vacuum Test Facility 2, which is 9.2 meters long, 4.9 meters in diameter and uses ten CVI TM1200i cryopumps to achieve a base pressure of 1.9×10^{-9} Torr¹⁰. The device center is located 1.2 meters from the chamber wall. Only two of the cryopumps are operated during this experiment, in order to decrease pumping speed so that the desired experimental pressures can be obtained using a 500 sccm- N_2 range MKS 1179A01352CS1BV mass flow controller. This mass flow controller is used to flow 99.999% argon into the chamber at a location approximately 1 meter away from the plasma device. Pressure is measured with $\pm 25\%$ accuracy¹¹ using a Bayard-Alpert 571 ionization gauge connected to the vacuum chamber with a Varian XGS-600 gauge controller, corrected for argon using a gas correction multiplier of 0.77.

A 4 inch diameter, 1/4 inch thick disc of HP grade boron nitride is positioned on centerline within the multipole plasma device using 1/4 inch OD alumina tubing

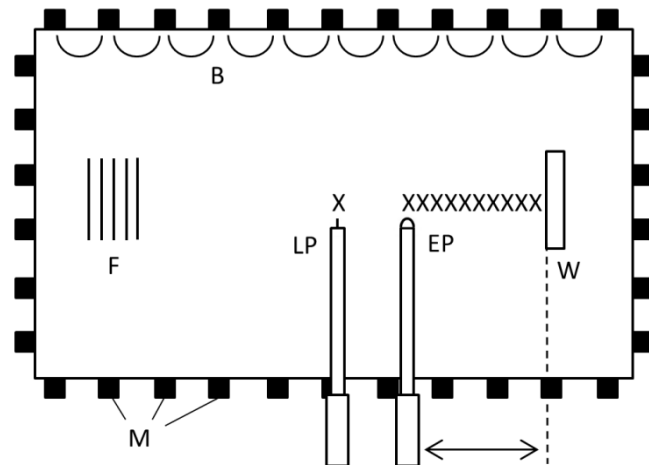


Figure 1. Schematic of experiment layout. *F* = filaments, *M* = magnets, *B* = nominal magnetic field, *LP* = Langmuir probe, *EP* = emissive probe, *W* = wall material sample, *X* = nominal data measurement location. Emissive probe orientation rotated 90° in figure to show hairpin tip geometry. Figure not to scale.

and the sheath potential profile is measured using an emissive probe as shown in Figure 1. The emissive probe is constructed of telescoping alumina tubing and a hairpin 0.005 inch diameter tungsten filament emissive tip. For the sheaths measured over the BN wall, plasma potential is measured using the separation point technique¹². A more precise emissive probe technique was employed for interpreting the alumina measurements (inflection point in the limit of zero emission.) This did have the disadvantage of increasing the time required to take measurements (~1 hour per potential profile), opening up measurements to the potential for error from fluctuations in the plasma or vacuum chamber conditions. Monitoring of chamber pressure did not show any pressure fluctuations while mass flow was held steady, or at least none that were visible with the resolution of the ion gauge controller readout which was $\pm 1 \times 10^{-6}$ Torr. Discharge current of the plasma cell exhibited drift and low-frequency oscillations on the order of 0.5 mA over 5 minutes, but this decreased to 0.1 mA over 5 min after approximately 20 minutes of operation at a condition. When drift occurred, discharge current was held constant by hundredth-amp adjustments to the filament heating current.

The emissive probe is positioned using a Parker 4062000XR linear motion table with a bi-directional repeatability of $\pm 5 \mu\text{m}$. The origin of the probe position is defined where the probe support touches the wall, which was determined with accuracy of $\pm 125 \mu\text{m}$. Bulk plasma parameters are measured using a cylindrical Langmuir probe constructed of alumina tubing with a 0.005 inch diameter tungsten tip of 0.20 inch length and interpreted using the orbital-motion-limited (OML) theory.

B. Simulation

Simulation of the experimental plasmas was performed using the plasma simulation code Starfish¹³. Starfish is a general 2D axisymmetric/Cartesian code which can be used to model a wide range of plasma and rarefied gas problems. Due to Starfish's broad range of capabilities, it is possible to simulate the current experiment in two different ways. The method selected is the simpler version, which is to simulate the domain near the wall with an ionized plasma interacting with the different wall materials. A linear Poisson solver is used, the overall potential drop is set to the experimental measured and the ion density is set equal to the experimentally measured value. The simulation is run until it reaches steady state to see the formation of the sheath.

III. Results and Discussion

A. Boron Nitride

The swept emissive measurements of plasma sheath potential profiles over the BN wall material sample are shown in Figure 2 for neutral pressures from 1×10^{-4} Torr-Ar to 5×10^{-5} Torr-Ar. The cylindrical Langmuir probe measurements of bulk plasma properties are displayed in Table 1.

The observed plasma potential profiles exhibit several deviations from the predictions of traditional collisionless sheath theory. The bulk plasma potentials of the experimental plasmas are negative, ranging from -12 V to -10 V. This effect is known to occur in multidipole plasmas at this pressure as reported in Ref. 14. In addition, the magnitudes of the potential differences across the measured sheaths are lower than would be predicted by traditional theory and the measured electron temperature. Also, the sheath width is larger by a factor of 5 than would be predicted by traditional theory and the measured electron density. It is believed that these deviations are due to high-energy electron populations present in multi-dipole devices.

Pressure	Electron Density	Electron Temperature	Sheath Voltage
(10^{-5} Torr-Ar)	(10^{14} m^{-3})	(eV)	(V)
10.0 ± 2.5	4.6 ± 1.1	1.23 ± 0.35	20.5 ± 2.0
7.5 ± 1.88	2.9 ± 0.7	1.66 ± 0.30	39.1 ± 3.5
5.0 ± 1.25	1.8 ± 0.4	2.16 ± 0.25	51.8 ± 2.4

Table 1. Langmuir probe measurements of bulk plasma parameters. OML theory used to interpret I-V curves.

Filament Bias	Electron Density	Electron Temperature	Sheath Voltage
(V)	(10^{14} m^{-3})	(eV)	(V)
-60 ± 0.25	3.5 ± 1.1	1.25 ± 0.35	38.8 ± 2.0
-70 ± 0.25	4.2 ± 1.1	0.95 ± 0.35	39.7 ± 2.0
-90 ± 0.25	3.6 ± 0.7	1.10 ± 0.30	8.5 ± 2.0
-120 ± 0.25	3.0 ± 0.4	1.15 ± 0.25	-2.6 ± 2.4

Table 2. Langmuir probe measurements of bulk plasma parameters. OML theory used to interpret I-V curves.

Shown in Figure 2, results of simulation demonstrate nominal agreement with experimental measurement, indicating that Starfish is able to correctly predict the variation in sheath potential profile.

B. Alumina

The swept emissive probe measurements of plasma sheath potential profiles over the alumina wall material sample are shown in Figure 2Figure 3 for neutral pressure of 7.5×10^{-5} Torr-Ar and filament bias voltages of -60, -70, -90, and -120 V. The cylindrical Langmuir probe measurements of bulk plasma properties are displayed in Table 2. Alumina is chosen in the hope that its increased SEE yield will enable experimental observation of the effect of SEE on sheath potential profile. The filament bias voltage is varied to increase electron temperatures and to increase electron power deposition to the alumina, and thereby increase SEE from the alumina surface.

As the negative bias voltage of the primary electrons is increased, it is seen that the sheath potential collapses as predicted by an increase in SEE. When the bias voltage has been increased to 120 V below the plasma device ground, the sheath has taken on the shape of an electron sheath, indicating the presence of significant SEE from the wall. In the intermediate cases, structure is observed that differs from the traditional Child-Langmuir profile that was observed with the BN samples, seemingly due to near wall space charge from the emitted electrons.

IV. Conclusion

The measurements and simulation presented in this article have shown that wall material selection and secondary electron emission properties can significantly affect the thickness of plasma sheaths as well as the magnitude of their overall potential difference from the bulk plasma, and represents steps toward development of an experimentally-validated simulation capability. The findings with alumina illustrate that the wall can play an important or even dominant role in the overall plasma power balance; as the filament bias voltage and primary electron energy is increased, the sheath disappears, from which it can be inferred that the alumina sample receives greatly increased power deposition from the plasma. This is mainly due to increased electron flux to the wall – without the potential barrier of the sheath to contain them in the plasma, the light and mobile electrons flow to the wall, depositing energy and limiting the electron and ion density achievable in the plasma. This is believed to be the mechanism responsible for the ion density saturation in HET discharge plasmas, and also believed to be the mechanism by which HETs walled with boron nitride have historically outperformed HETs walled with alumina.

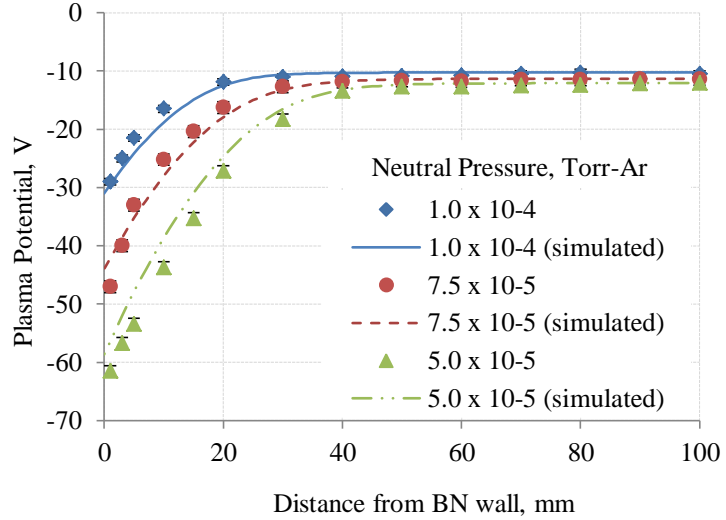


Figure 2. Measurements of sheath potential profile over BN surface. Pressures are 5×10^{-5} , 7.5×10^{-5} , and 1×10^{-4} Torr-Ar and for all cases filaments are biased to -87 V and frame is grounded (0 V) with 9.5 mA discharge current.

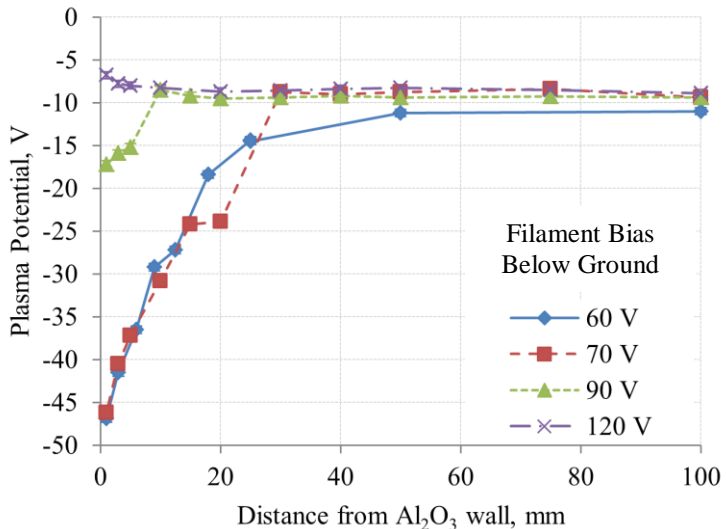


Figure 3. Measurements of sheath potential profile over alumina surface. For all cases, neutral pressure is 7.5×10^{-5} Torr-Ar with 10.0 mA discharge current.

Acknowledgments

This work is supported by the Air Force Office of Scientific Research through Grant FA9550-11-10160.

References

- ¹Brown, D. L., "Investigation of Low Discharge Voltage Hall Thruster Characteristics and Evaluation of Loss Mechanisms," Ph.D. Dissertation, University of Michigan, 2009.
- ²Raitses, Y., et al. "Measurements of secondary electron emission effects in the Hall thruster discharge." *Physics of Plasmas* 13 (2006): 014502.
- ³Campanell, M. D., Khrabrov, A. V., and Kaganovich, I. D. "Absence of Debye Sheaths due to Secondary Electron Emission." *Physical Review Letters* 108.25 (2012): 255001.
- ⁴Hershkowitz, N. "Sheaths: More complicated than you think." *Physics of plasmas* 12 (2005): 055502.
- ⁵Oksuz, L., and N. Hershkowitz. "Plasma, presheath, collisional sheath and collisionless sheath potential profiles in weakly ionized, weakly collisional plasma." *Plasma Sources Science and Technology* 14.1 (2005): 201.
- ⁶Lee, D., Severn, G., Oksuz, L., and Hershkowitz, N. "Laser-induced fluorescence measurements of argon ion velocities near the sheath boundary of an argon-xenon plasma." *Journal of Physics D: Applied Physics*, 39(24), (2006): 5230.
- ⁷Limpaecher, Rudolf; Mackenzie, K.R., "Magnetic Multipole Containment of Large Uniform Collisionless Quiescent Plasmas," *Review of Scientific Instruments*, vol. 44, no. 6, pp. 726-731, June 1973.
- ⁸Lang, Alan and Noah Hershkowitz. "Multidipole plasma density." *J. Appl. Phys.* 49, 4707 (1978)
- ⁹Leung, K. N., T. K. Samec, and A. Lamm. "Optimization of permanent magnet plasma confinement." *Physics Letters A* 51.8 (1975): 490-492.
- ¹⁰Kieckhafer, A. W., and Walker, M. L. R., *Proceedings of the 32nd International Electric Propulsion Conference*, "Recirculating Liquid Nitrogen System for Operation of Cryogenic Pumps", Hamburg, Germany, September 2011.
- ¹¹Stanford Research Systems, Appl. Note "Bayard-Alpert Ionization Gauges", pp. 38, <http://www.thinksrs.com/downloads/PDFs/ApplicationNotes/IG1BAGapp.pdf> [cited 1 July 2013].
- ¹²Sheehan, J. P., et al. "A comparison of emissive probe techniques for electric potential measurements in a complex plasma." *Physics of Plasmas* 18 (2011): 073501.
- ¹³Brieda, L., and Keidar, M., "Development of the Starfish Plasma Simulation Code and Update on Multiscale Modeling of Hall Thrusters", *48th AIAA Joint Propulsion Conference*, Atlanta, GA, 2012.
- ¹⁴Oksuz, L., and Hershkowitz, N. "Negative plasma potential in unmagnetized DC electropositive plasma with conducting walls." *Physics Letters A* 375.22 (2011): 2162-2165.